Nonequilibrium dynamics of a hadronizing quark-gluon plasma[1]

M. Hofmann[a], J. M. Eisenberg[b], S. Scherer[a], M. Bleicher[a,2], L. Neise[a], H. Stöcker[a], W. Greiner[a]

[a] *Institut für Theoretische Physik, J. W. Goethe-Universität, D-60054 Frankfurt am Main, Germany,*
[b] *School of Physics and Astronomy, Tel Aviv University, 69978 Tel Aviv, Israel*

Abstract

We investigate the hadronic cooling of a quark droplet within a microscopic model. The color flux tube approach is used to describe the hadronization of the quark phase. The model reproduces experimental particle ratios equally well compared to a static thermal hadronic source. Furthermore, the dynamics of the decomposition of a quark-gluon plasma is investigated and time dependent particle ratios are found.

1 Introduction

When the possible existence of a quark-gluon plasma was first postulated in the mid seventies [1] several groups started to investigate unique signatures which would allow the identification of such a gas of asymptotically free quarks and gluons in heavy ion collisions. Tightly connected to this task was the study of the mechanism for the decomposition of a once formed partonic state of matter, back to the hadronic world measured in detectors. One was immediately lead to the question of the order and signatures of a QGP-hadron phase transition. Under the widely used assumption of a first order transition a sharp surface of the quark phase could be defined at which the hadronization should take place. Applying Gibbs conditions at the phase boundary then gives a macroscopic view

[1] This work was supported by BMBF, DAAD, DFG, GSI, Graduiertenkolleg Theoretische und Experimentelle Schwerionenphysik, and the A. v. Humboldt Foundation.

[2] Fellow of the Josef Buchmann foundation

on the properties of the initial quark and the final hadron phase. However, the dynamical aspects of the plasma disassembly (e. g. the dissociation rate) could not be tackled in this simple picture.

Therefore, several different models for the dynamics of the transition were proposed which all focused on the radiation of hadrons from the plasma surface. One of these contributions was driven by our late friend Judah Eisenberg [2] who proposed a quark-gluon bag which was surrounded by a cloud of pions. Both phases interact at the phase boundary via the coupling of the pseudoscalar pion field to the quark vector-field in the interior of the bag. However, this and other similar approaches as e.g. [3] still lacked a dynamical description of the conversion process and therefore seemed to be restricted to stationary problems in equilibrium. This problem was partially attacked by the application of the color flux tube model to the radiation scenario as proposed in [4]. Here, the idea of confinement is adopted to describe hadronization dynamics. Now a dynamical non-equilibrium calculation of the pion production rates was possible. However, all those approaches predicted that the contribution of surface radiation to the total hadron yield in heavy ion collisions should be small compared to the strong hydrodynamic expansion of a hot fireball. Even the extension of the flux tube model to four quark flavors and the complete hadron zoo could not circumvent this result.

Nevertheless, the hadron radiation process is yet not completely negligible which is underlined by the rough accordance of all those different models within one order of magnitude (fig. 1). But, evidently, the dynamics of the phase transition cannot be separated from the dynamics of the QGP phase itself which includes the radiation from the surface as well as the expansion. The latter, however, requires a new, dynamical definition of the "surface" of a QGP as this surface will now be time dependent. In the microscopic picture of moving quarks (as the flux tube model) a surface cannot be defined consistently: it has to be introduced "by hand" as a boundary condition. The complete microscopic description will therefore not contain such a surface. Inspired by Judah Eisenberg we extended the flux tube approach by assuming the confining force acting on an escaping quark as dynamically induced by all the other quarks which define the plasma phase, i. e. one quark moves in the effective color field of all the others.

This paper presents this model to describe the dynamics of the hadronization transition. It explicitly takes into account a non-equilibrium evaporation scenario.

2 Hadron radiation from quark-gluon plasma

Two fundamental scenarios have been suggested for the decay of a quark-gluon plasma within the past fifteen years. The first scenario assumes a hydrodynamical expansion of the plasma and a cooling which leads to hadronization [5]. In a second approach hadronization is constrained to the plasma surface mediated by a particular interaction between the two phases. Several hypotheses have been developed, all of which assume an equilibrated plasma state that evaporates mesons according to specific mechanisms. Reciprocally, the plasma should also be able to absorb hadrons from outside with a certain probability.

The pion emission rate of a thermalized quark gas has been calculated [3] by introducing a fixed threshold quark momentum for the hadronization of escaping quarks to pions. Thus the pion yield is determined by the characteristics of the initial plasma state, and the energy flux of pions per unit time and surface element $\mathrm{d}^3E/\mathrm{d}^2S\,\mathrm{d}t$ obeys a Stefan-Boltzmann T^4 law.

A more sophisticated mechanism of meson evaporation from a plasma state uses the cloudy-bag model postulating the existence of a pseudo scalar pion field outside the plasma region coupled to the quarks at the surface [2]. In this model pions are produced by the processes $q \to q\pi$, $\bar{q} \to \bar{q}\pi$ and $q\bar{q} \to \pi$ at the surface of the bag. The result of this model differs drastically from the predictions of [3], revealing an approximate power law for the emissivity of T^6.

In this paper we apply a hadronization scheme proposed by Banerjee et al. [4]. A quark penetrating the bag surface is pulled back by a strong color interaction with the volume of the plasma. The confining force increases with the distance from the plasma so that a quark cannot escape. This attractive potential is simulated by a color flux tube connecting the emitted quark to the plasma by a uniform color field. This tube can decay by creation of virtual $q\bar{q}$ pairs inside the color field. The color charges of the pair produce screening of the color field between the initially emitted quark and the quark droplet and allow q and $\overline{q}$ to build a color singlet state (a meson). The remaining q will be trapped in a color flux tube again.

Baryon production can be implemented e. g. by inclusion of (anti-)diquark states (uu, ud, ...) which later may combine with a single quark to form a baryon. However, the probability for $qq - \overline{qq}$ production is strongly suppressed by the relatively large masses of the diquark states, so that the predicted baryon multiplicities underestimate the experimental result. Therefore, our calculation treats diquarks as constituents of the quark-gluon plasma. This mechanism will drastically increase the number of emitted baryons.

The existence of bound diquarks states in the QGP conflicts with the expectations of an asymptotically free quark-gluon plasma. However, recent cal-

culations of several groups hint at the existence of correlations in the QGP even for $T \leq 2T_C$.

We assume that a quark-gluon plasma bag has a radius of $R \sim 2 - 6\,\mathrm{fm}$ and is in complete thermal and chemical equilibrium at temperatures $T \sim 100 - 250\,\mathrm{MeV}$. It is filled with asymptotically free quarks and antiquarks. In the following we neglect the gluonic degrees of freedom.

Let us consider a thermal quark plasma bag with a sharp surface. This state will then radiate hadrons from the surface which change the energy and flavor content of the plasma. We consider that near the surface the particles are homogeneously distributed in space, while their momentum distribution is approximated by the Boltzmann distribution $\exp(-\sqrt{p^2 + m_q^2}/T)$. We assume to have current quarks (and diquarks) inside the plasma. In this approximation the mean particle number for each species q inside the bag is

$$N_q(T, V, \mu) = g_q \, e^{\mu/T} \, \frac{V}{2\pi^2} m_q^2 \, T \, K_2 \left(\frac{m_q}{T} \right) \, , \tag{1}$$

where q runs over all possible (anti-)quark and (anti-)diquark states, and g_q is the degeneracy factor which counts all possible color and spin states.

In contrast to the other models of hadron radiation cited in this article, we are, in principle, *not* restricted to a thermal initialization of the plasma phase.

2.1 Hadronization via fission of color flux tubes

The string mechanism proposed in [6] describes the fragmentation of a color flux tube created between two point-like quarks excited by a high impact $p + p$ (or heavy ion) collision. It is assumed that longitudinal momenta of quarks are much higher than the transverse components so that a $1 + 1$ dimensional description is appropriate. A string stretched between a quark and a large bag is different since the color field is not necessarily constrained to a tube. However, assuming free motion of color charges on the surface of the bag, we assume a flux tube which is perpendicular to the bag surface and will follow a possible quark motion perpendicular to the tube.

A quark crossing the surface of the bag travels outward in accordance with the attractive potential of the color flux tube. In $1+1$ dimensions this potential is taken to be linear

$$V(z) = \kappa \cdot z \, , \tag{2}$$

which assumes a constant chromoelectric field strength density $\mathrm{d}V/\mathrm{d}z = \kappa \approx 0.9\,\mathrm{GeV/fm}$. This value can be extracted from fits to Regge trajectories or from lattice calculations [7].

The total probability of vacuum decay is then given by

$$p = \sum_{f=q,qq} p_f \,, \qquad p_f = \frac{\kappa}{4\pi^3} \sum_{n=1}^{\infty} \frac{1}{n^2} \, e^{-\frac{\pi m_f^2 \, n}{\kappa}} \,, \tag{3}$$

where the sum runs over all quarks and diquarks, p_f is the probability per unit four-volume to produce a virtual $q_f \bar{q_f}$ pair in a constant field [8, 9] , and m_f is the mass of the produced quarks (or diquarks). The total probability of vacuum decay is then given by This result has the same form as Schwinger's formula for e^+e^- production in an constant external field [10]. Nevertheless, it should be noted that the above result is valid only for a static, homogeneous color field, i. e. for a flux tube with infinite transverse dimensions. Finite flux tubes impose surface effects which may noticeably modify the field configuration and pair production probabilities. In [11] it was shown that a string radius of 0.5 fm reduces the pair creation rate by about 40%.

For the quark masses we assume the following values of $m_u = m_d = 5\,\mathrm{MeV}, m_s = 150\,\mathrm{MeV}, m_c = 1.5\,\mathrm{GeV}$. For the mass of the diquarks two different possibilities are taken into account: masses derived from fits to experimental e^+e^- data which allow to extract a probability ratio $p(qq)/p(q) = 0.065$ for diquark production [12], and, secondly, diquark masses calculated within the Nambu-Jona-Lasinio model [13]. One obtains different masses for different flavor and spin combinations. Combining u, d and s flavors and using simple symmetry arguments for the diquark wave functions (see e.g.[14]) one obtains three antisymmetric diquark states of spin 0

$$(ud)_0 = \frac{1}{\sqrt{2}}(ud - du), \quad (us)_0 = \frac{1}{\sqrt{2}}(us - su), \quad (ds)_0 = \frac{1}{\sqrt{2}}(ds - sd) \,, \tag{4}$$

and six symmetric combinations

$$(uu)_1 = uu, \quad (ud)_1 = \frac{1}{\sqrt{2}}(ud + du), \quad (dd)_1 = dd, \tag{5}$$

$$(ss)_1 = ss, \quad (us)_1 = \frac{1}{\sqrt{2}}(us + su), \quad (ds)_1 = \frac{1}{\sqrt{2}}(ds + sd) \,, \tag{6}$$

with spin 1. Since only the anti-triplet representation of the $SU(3)_c \times SU(3)_c$ may contribute to a diquark state, we obtain a color degeneracy of 3. Considering all the spin and isospin combinations, we arrive at the total degeneracy factors for each kind of diquarks given in table 1.

	$(qq)_0$,$(\bar{q}\bar{q})_0$	$(qq)_1$,$(\bar{q}\bar{q})_1$	$(qs)_0$,$(\bar{q}\bar{s})_0$	$(qs)_1$,$(\bar{q}\bar{s})_1$	$(ss)_1$,$(\bar{s}\bar{s})_1$
LUND mass (MeV)	420	490	590	640	790
NJL mass (MeV)	234	822	537	962	1087
degeneracy	3	27	6	18	9

Table 1: Diquark degeneracies and masses. Masses are taken from fits to the LUND string model and from calculations within the NJL model.

Assuming a string cross section A and a constant break-up probability p inside the string volume we obtain a time-dependent probability for string fission

$$P(t) = 1 - e^{-p\,A\int_0^t \mathrm{d}t'\, z(t')} \tag{7}$$

where $z(t)$ is the distance of the quark from the surface. The flavor of the created quarks and therefore the species of the hadron to be produced is chosen according to the probability given by (3), defining all quantum numbers. If this choice proves to be energetically impossible the produced flavor will be reselected. The remaining quark is propagated within the attractive color potential from the position of the point of break-up until the flux tube breaks up again or the quark is pulled back into the plasma. String fission is only possible while the quark is moving outward ($p_q^z > 0$).

The flavor and the quantum numbers of the produced $q\overline{q}$ (or $qq - \overline{qq}$) pair determine the species of the produced hadron. Quantum mechanical binding properties have been neglected as well as possible mass reduction of the hadrons due to the dense surrounding medium. Thus the free vacuum mass for the hadrons is assumed. The probability for the $q\overline{q}$ pair to have a transverse momentum $p_\perp$ is

$$P(p_\perp) = e^{-\frac{\pi E_\perp^2}{\kappa}} \qquad \text{with} \quad E_\perp = \sqrt{M^2 + (P_M^\perp)^2}\,. \tag{8}$$

From momentum conservation during the string fission we obtain directly the transverse momentum of the meson. The longitudinal hadron momentum is determined by using the fragmentation function f according to [15, 6, 16]

$$z\, f(z) \sim (1-z)^\alpha\, e^{-\beta\, E_\perp^2/z}\,, \tag{9}$$

where $z = p_{\mathrm{hadron}}/p_{\mathrm{initial\,quark}}$ and α, β are free parameters which are fixed in the LUND model to $\alpha = 1$ and $\beta = 0.7\,\mathrm{GeV}^{-2}$.

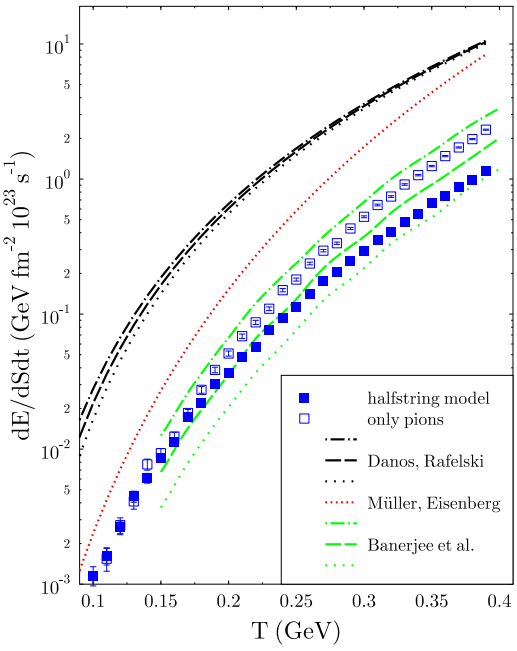

Figure 1: Pion surface brightness of a baryon-free QGP as a function of temperature. Three upper lines are the results from Danos and Rafelski [3], the dotted line are calculated by Müller and Eisenberg [2] while the three lower lines represents the results from Banerjee et al. [4] for various model parameters. The filled squares are the calculations with inclusion of all hadrons species while the open squares give the results, when only pion production is taken into account.

2.2 Results

Figure 1 shows the surface brightness $\mathrm{d}^3E_\pi/\mathrm{d}S\,\mathrm{d}t$ of the pion radiation as function of temperature T. We compare predictions of three different models by Danos and Rafelski [3] (upper lines), Müller and Eisenberg [2] (dotted line) and Banerjee et al. [4] (lower lines) with our results. We predict the same orders of magnitude as in [4]. The bending of the curve increases heavily with increasing temperature which is due to the opening of new hadronic degrees of freedom at higher energies. To see this, we recalculated the distribution neglecting all hadrons other than pions (□) which then gives a good agreement to the former results.

As describes so far, our model assumes a static plasma source. It has been shown in ref. [17] that hadron ratios change with time, i. e. during the reaction some particle species are produced earlier than others. Furthermore, the hadron evaporation in each time step will influence the statistical properties of both the plasma phase and the hadronic phase. This dynamical evolution will pull the system from an initial $f_s = 0$ into a domain of finite strangeness in both phases [17].

It is interesting that the model is able to reproduce experimental data fairly

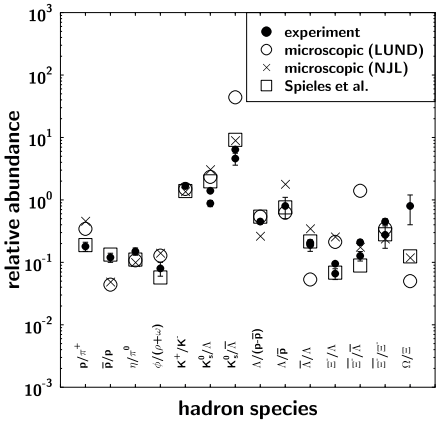

Figure 2: Final particle ratios in the non-equilibrium scenario with initial conditions $A_B^{\rm init} = 100$, $S/A^{\rm init} = 45$, $f_s^{\rm init} = 0$, $B^{1/4} = 235\,{\rm MeV}$ corresponding to the calculations in [17] (squares). The circles represent the results assuming LUND diquark masses [16], while the crosses denote calculations for diquark masses extracted from the NJL model [13]. Data from various experiments as compiled in [18] are also shown.

good even in a static approach, as can be seen in fig. 2. The initial conditions of the plasma phase have been chosen to be equivalent to those used in [17] $A_B^{\rm init} = 100$, $S/A^{\rm init} = 45$, $f_s^{\rm init} = 0$, $B^{1/4} = 235\,{\rm MeV}$. The NJL diquark masses seem to reproduce the experimental data better than LUND masses. This is not surprising, since the LUND masses have been extracted from fits of the string model to high energy data ($\sqrt{s} \approx 4\,{\rm GeV}$) while average quark momenta in our scenario are certainly below 1 GeV.

One sees that our calculations fit the data almost as well as the dynamical model and are in accordance to a static thermal fit. This is ensured by the inclusion of diquarks in our plasma. First, they are responsible for creating baryon numbers but secondly they reduce the distill effect of net strangeness. Indeed, at finite μ_q an excess of q compared to $\overline{q}$ leads to enhancement of $\overline{s}$ and therefore K^+ in the hadronic phase. The qq and qs diquarks also exceed the number of $\overline{qq}$ and $\overline{qs}$ (suppressed) diquarks, but the latter may now combine with a s to form a Λ, Σ or Ξ. This then leads to an enhancement of s in the hadronic phase. The net strangeness enrichment in the hadronic sector is therefore balanced by the diquark contribution which is mostly influenced by the initial baryon chemical potential μ_q.

This is illustrated in fig. 3 where the strangeness fraction $f_s = (N_s - N_{\overline{s}})/A$ is plotted as a function of the chemical potential μ_q for $\mu_s = 0$ (diamonds) and $\mu_s = 25\,{\rm MeV}$ (circles). For small μ_q diquark production in the plasma is suppressed due to the high diquark masses and therefore $\overline{s}$ is enriched on the hadronic phase giving rise to negative f_s. For higher μ_q the strangeness fraction goes to zero which indicates that both effects almost cancel. At $\mu_q \to 0$ there should be $f_s = 0$ due to restoration of baryon number symmetry. From the

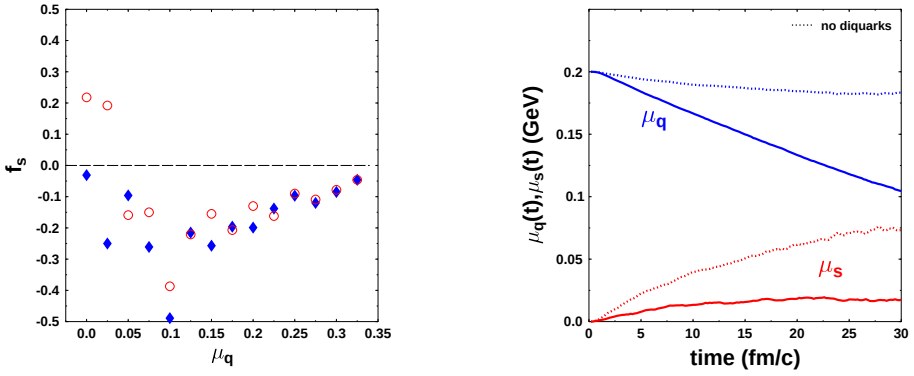

Figure 3: (Left) Strangeness fraction $f_s = (N_s - N_{\overline{s}})/A$ as a function of initial baryon chemical potential μ_q from microscopic calculation for $\mu_s^{\rm init} = 0$ ($\diamond$) and $\mu_s^{\rm init} = 25\,{\rm MeV}$ ($\bigcirc$). (Right) Time evolution of chemical potentials μ_q and μ_s assuming a totally equilibrated plasma phase at every stage of the reaction with an initial temperature $T = 190\,{\rm MeV}$. The dashed lines give the respective μ's for a plasma without diquarks.

microscopic calculation it is not clear whether there is a smooth transition in f_s from finite μ_q to $\mu_q = 0$ or a discontinuity as net strangeness and baryon numbers converge to zero. The large deviation of two points at small μ_q indicate a significant uncertainty in this observable.

For small but finite initial μ_s we observe a positive f_s for small μ_q, as it can be expected. For higher μ_q the described $\overline{s}$ transport mechanism becomes more important and finally dominates the initial strangeness excess.

From fig. 3 (left) it is obvious that one feature of a dynamical treatment of hadronization cannot be described in a static scenario: the accumulation of anti-strangeness in the hadronic phase causes an excess of strangeness inside the plasma which will then change the strange chemical potential to finite $\mu_s > 0$. The energy stuffed into strangeness will then cause a strong reduction of μ_q. Figure 3 (left) shows that for $\mu_q > 50$ MeV this will cause an even higher strangeness enrichment. For small μ_q, on the other hand, the growing μ_s will finally pull the system in a domain of positive f_s, which means s-dominance in the hadronic phase which can no longer be compensated by the small baryon chemical potential.

Fig. 3 (right) elucidates this scenario. The time evolution of μ_s and μ_q is plotted for initial conditions $T = 190\,{\rm MeV}$, $\mu_q^{\rm init} = 200\,{\rm MeV}$ and $\mu_s^{\rm init} = 0$ for both a plasma with (solid lines) and without (dotted lines) initial diquarks.

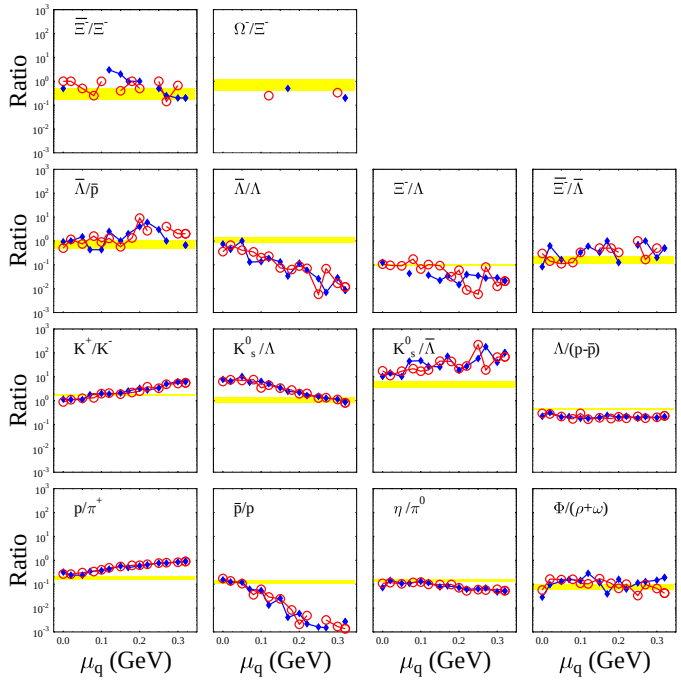

Figure 4: Hadron ratios as a function of μ_q for $\mu_s = 0$ ($\diamond$) and $\mu_s = 25\,\mathrm{MeV}$ ($\bigcirc$). The grey bars indicate the experimental data including error bars.

The time dependence is obtained by adjusting the thermodynamical conditions inside the plasma to the average baryon number, strangeness and energy transport through the plasma surface calculated by the microscopic model for given initial conditions. The assumption of a complete statistical equilibrium of the plasma after each time step allows to extract new parameters μ_q, μ_s (as we are treating only particle rates the volume V of the plasma is of no importance for particle ratios, unlike the absolute number of produced hadrons which is proportional to the plasma surface). The temperature is assumed to be constant. It is worth to note that in this scenario we do not need to require equilibration for the hadronic phase or validity of Gibbs conditions at the transition. Thus, our model is a non-equilibrium description of the hadronization procedure.

In absence of diquarks in the plasma the strange chemical potential monotonically rises with time. This is in agreement to the results of ref. [17]. If

diquarks are taken into account the picture changes drastically. After a short period the μ_s contribution saturates at about 25 MeV. On the contrary the μ_q distribution decreases linearly in time which gives possibility to use μ_q as a time evolution parameter. The strangeness distillery is strongly reduced by including diquarks.

Finally, fig. 4 shows the μ_q dependence of different particle ratios compared with experimental data for $\mu_s = 0$ and $\mu_s = 25\,\mathrm{MeV}$, where the latter represents the saturation value for μ_s in the time dependence. Within the statistical fluctuations of the ratios, the two curves cannot be distinguished. Therefore, the distributions may be viewed as some kind of time evolution of the particle ratios.

3 The quark molecular dynamics (qMD)

A novel extension of the quark dynamics can be realized by treating quarks as semi-classical particles which interact according to a two-body color potential (for details see [21]). This potential is phenomenologically motivated in order to mimic the soft gluonic part of a quark-gluon plasma. The Hamiltonian reads

$$\mathcal{H} = \sum_{i=1}^{N} \sqrt{p_i^2 + m_i^2} + \frac{1}{2} \sum_{i,j} C_{ij}^c V(|\mathbf{r}_i - \mathbf{r}_j|)$$

where N is the number of quarks. Here we include four quark flavors (u, d, s, c) with current masses $m_u = m_d = 10\,\mathrm{MeV}$, $m_s = 150\,\mathrm{MeV}$ and $m_c = 1.5\,\mathrm{GeV}$.

C_{ij}^c indicates the color factor which regulates the sign and relative strength of the interaction between any two quarks and antiquarks depending on the color combination of each pair. They can easily be obtained from the quark-gluon vertex factors in color space and read

$$C_{\alpha\beta}^c = \sum_{a=3,8} \lambda_{\alpha\alpha}^a \lambda_{\beta\beta}^a$$

in the abelian approximation. This yields e. g.

$$C_{RR}^c = -1\,, \qquad C_{RG}^c = +\frac{1}{2}\,, \qquad C_{R\overline{R}}^c = +1\,, \qquad C_{\overline{R}G}^c = -\frac{1}{2}\,.$$

It is worth to note that the relative strength of the above color factors is rigorously enforced by the requirement of color neutrality of widely separated $q\overline{q}$ and qqq states.

To provide confining properties $V(r)$ is taken to be linear at large distances. At short distances the strong coupling constant α_s becomes small compared to 1 which causes the one-gluon exchange terms to dominate the interaction and therefore induces a coulomb-like potential. In total, one obtains the well known Cornell-potential [22]

$$V(r) = -\frac{3}{4}\frac{\alpha_s}{r} + \kappa\, r \ .$$

In the static case of infinite quark masses this interquark potential has been confirmed by lattice calculations over a wide range of quark distances [7].

The second request to the model is to define a criterion how to map those bound quark states to hadrons. Such a mechanism is essential as the Hamiltonian is not tuned to describe bound and truly confined hadron states. This has been done by the requirement that the total color interaction from a pair (or a three particle state) of quarks with the remaining system vanishes. Then, these $q\overline{q}$- and qqq-states do no longer contribute to the color interaction of the quark gas. If a bound quark state fulfills the hadronization criterion it will be mapped to an appropriate hadronic state with identical quantum numbers. Spin and isospin of the hadron is randomly chosen according to the probabilities given by the Clebsch-Gordon coefficients while the mass of the produced hadron is determined by energy and momentum conservation.

3.1 Dynamics of the model

We can now study the dynamical evolution of the system. We use the Metropolis algorithm to generate a thermal distribution of quarks where longitudinally, a Bjorken-like velocity profile $v_z = z/t$ has been imposed.

Within about $12\,\mathrm{fm}/c$ most of the initial quarks are completely hadronized. It becomes obvious that this hadronization process is *not* compatible to a radiating hadron source, but is ruptured into several small quark blobs before finally dissolving.

As the geometry of the quark phase resembles those of an assumed fireball in a S+Au collision, we compare in fig. 5 the calculated hadron yields at mid-rapidity to those measured in CERN-SPS experiments (see compilation in [18]). We find a very good agreement in all MM, MB and BB ratios, while the antibaryons seem to be clearly under-predicted. Particle ratios, however, proved not to be a very sensitive observable to test the quality of theoretical models. Fits of a pure hadron gas [18] proved to describe data with a comparable precision as other thermal or hydrodynamical approaches including a QGP phase transition or several microscopic simulations as UrQMD [19]. However, the analysis of event-by-event fluctuations [20] and of the dynamical properties

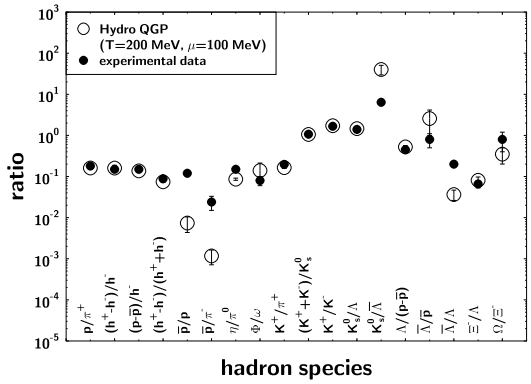

Figure 5: Final state hadron ratios from qMD calculations (open circles) compared to S+Au data at 200 AGeV (full circles, taken from [18]).

of the system may yield new insight. Thus, we shall further scrutinize the dynamical properties of the qMD approach. As the initial conditions were taken from the idealized Bjorken scenario we shall focus to the transverse dimension at mid-rapidity. Fig. 6 (right) depicts the transverse mass spectra of various hadron species as produced by qMD with the above initial conditions. The distribution of the initialized quarks (left part) shows $T = 200\,\mathrm{MeV}$ for all u, d and s-quarks and underlines the initialization procedure. In the final curves, however, we observe a significant dependence of the slope of the distribution from the mass of the regarded hadron species. We stress again that no transversal flow had been imposed. This result is in strong contrast to the fireball model proposed in [23] which explicitly required a transverse velocity profile in order to obtain such transversal behavior.

4 Conclusion

Experimental particle ratios at SPS energies had been shown to be compatible with the scenario of of a static, thermally and chemically equilibrated hadron gas. The present paper demonstrates that the experimental data are also compatible with a scenario with a quark gluon plasma consecutively evaporating hadrons, provided that the plasma contains thermally distributed bound diquark states. Without diquarks the model fails to describe the observed baryon abundances. Neither a bag constant nor equilibration of the hadronic phase is assumed in this model.

Under the assumption that the plasma phase itself remains equilibrated during the reaction, a quasi time evolution of the plasma blob can be determined. The model predicts strangeness distillation in the quark-hadron transition. The

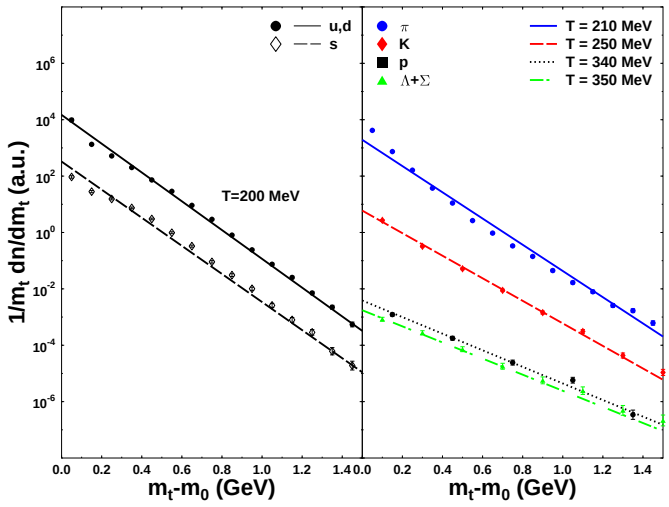

Figure 6: (Left) Transverse mass spectra of the initial thermalized u, d (circles) and s-quarks (open diamonds). Both distributions show $T = 200$ MeV as initialized. (Right) Transverse mass spectra of final π, K, p and Λ in arbitrary units. One obtains rising inverse slope parameters with increasing particles masses.

inclusion of diquarks reduces the strangeness enhancement.

The extension of the model to non-equilibrium initial conditions results in a proper description of the transverse and longitudinal expansion with a good agreement of the hadro-chemical properties.

References

[1] J.C. Collins and M.J. Perry, *Phys. Rev. Lett.* **34**, 1553 (1975) ; A.M. Polyakov, *Phys. Lett.* B **72**, 224 (1977)

[2] B. Müller, J. M. Eisenberg, *Phys. Rev. Lett.* **52**, 1590 (1984)

[3] M. Danos, J. Rafelski, *Phys. Rev.* D **27**, 671 (1977)

[4] B. Banerjee, N. K. Glendenning, T. Matsui, *Phys. Lett.* B **127**, 453 (1983)

[5] J. D. Bjorken, *Phys. Rev.* D **27**, 140 (1983)

[6] B. Andersson, G. Gustafson, C. Peterson, *Nucl. Phys.* B **135**, 273 (1978)

[7] K. D. Born, E. Laermann, R. Sommer, T. F. Walsh, P. M. Zerwas, *Phys. Lett.* B **329**, 325 (1994)

[8] A. Casher, H. Neuberger, S. Nussinov, *Phys. Rev.* D **20**, 179 (1979)

[9] N. K. Glendenning, T. Matsui, *Phys. Rev.* D **28**, 2890 (1983)

[10] J. Schwinger, *Phys. Rep.* **82**, 664 (1951)

[11] T. Schönfeld, A. Schäfer, B. Müller, K. Sailer, J. Reinhardt, W. Greiner, *Phys. Lett.* B **247**, 5 (1990)

[12] K.W. Bell, B. Foster, J.C. Hart, J. Proudfoot, D.H. Saxon, P.L. Woodworth, Rutherford preprint **RL-82-011** (1982)

[13] U. Vogl, W. Weise Prog. Part. Nucl. Phys. **27**, 195 (1991)

[14] M. Szczekowski, Int. J. Mod. Phys. A **4**, 3985 (1989)

[15] R. D. Field, R. P. Feynman, *Phys. Rev.* D **15**, 2590 (1977)

[16] B. Andersson, G. Gustafson, G. Ingelman, T. Sjöstrand, *Phys. Rep.* **97**, 31 (1983)

[17] C. Spieles, H. Stöcker, C. Greiner Eur. Phys. J. C **2**, 351 (1998)

[18] P. Braun-Munzinger, J. Stachel, J.P. Wessels, N. Xu, *Phys. Lett.* B **344**, 43 (1995); P. Braun-Munzinger, J. Stachel, J.P. Wessels, N. Xu, *Phys. Lett.* B **365**, 1 (1996); P. Braun-Munzinger, J. Stachel, *Nucl. Phys.* A **606**, 320 (1996).

[19] S.A. Bass, M. Belkacem, M. Brandstetter, M. Bleicher, L. Gerland, J. Konopka, L. Neise, C. Spieles, S. Soff, H. Weber, H. Stocker, W. Greiner *Phys. Rev. Lett.* **81**, 4092 (1998)

[20] M. Bleicher, M. Belkacem, C. Ernst, H. Weber, L. Gerland, C. Spieles, S. A. Bass, H. Stöcker, W. Greiner *Phys. Lett.* B **435**, 9 (1998)

[21] M. Hofmann, M. Bleicher, S. Scherer, L. Neise, H. Stöcker, W. Greiner, submitted to *Phys. Lett.* B

[22] E. Eichten *et al.*, *Phys. Rev. Lett.* **34**, 369 (1975)

[23] K. S. Lee *et al.*, *Z. Phys.* C **48**, 525 (1990)